Computational Particle Mechanics
https://doi.org/10.1007/s40571-021-00446-6

An extension of the Fourier series-based particle model to the GJK-based contact detection and resolution framework for DEM

Shuai Huang[1] · **Linchong Huang**[2] · **Zhengshou Lai**[1,3]

Received: 30 June 2021 / Revised: 15 October 2021 / Accepted: 25 October 2021

Abstract
Fourier series (FS) is an efficient tool for describing irregular geometries and has been employed to develop the FS-based particle model in the discrete element method (DEM). This work is devoted to extending the previous FS-based particle model to the Minkowski and Gilbert–Johnson–Keerthi (GJK)-based contact detection and resolution framework for DEM, and thus to improving its computational efficiency and compatibility with other conventional particle models. In the new FS-based particle model, instead of representing particle surface, the FS is proposed to represent the support function of particle surface. Particle surface and support points are then formulated based on the FS support function. As the Minkowski- and GJK-based detection and resolution framework relies heavily on the convexity of particles, the convexity constraint and the approach to generate convexity preserving FS-based particles are also presented. The accuracy of the new FS-based particle model for shape representation is analyzed using a set of irregular shape templates. DEM simulation of random packing and biaxial compression test with various particle models is also performed to demonstrate the computational performance and numerical stability of the new FS-based particle model.

Keywords Discrete element model · Irregular shapes · Fourier series · GJK · Convexity preserving

1 Introduction

The discrete element method (DEM) [1] is a type of discontinuous mechanical method that is suitable for modeling granular materials. It has been applied to study material anisotropic behavior [2,3], stability and localization problems [4,5], dry and saturated granular flows [6], and also in multiscale simulations [7,8]. In order to approach accurate modeling of granular materials based on DEM, it is critical to precisely incorporate the particle physical and morphological features into the DEM model. In particular, particle shape is known as a salient factor that would affect the bulk behavior of a granular material. It could make a significant contribution to the porosity, compressibility, critical state line intercept and, etc., of granular packing [9,10]. Thus, the research on developing irregular-shaped particle models for accurate and efficient DEM simulations has been attracting increasing interests recently.

Geometrically, any concave shapes can be decomposed into pieces of convex shapes, which thus can be regarded as the primary elements/shapes in DEM and will be the focus of this study. In two dimensions, particle models have been developed using ellipse [11], polygon [12], NURBS [4,13], Fourier series (FS) [14,15], polybézier [16], and, etc. Reviews on the developments of particle models can be seen in Lu et al. [17], Zhong et al. [18]. Among the various particle models, the FS-based particle model is attractive due to the reasons in twofold. First, benefiting from the characteristics of FS, the FS-based particle model is able to describe general irregular-shaped particles with high accuracy and efficiency [19,20]. Second, there have been researches showing that the morphological characteristics (e.g., elongation, roundness and roughness) of a particle could be related to the FS coefficients, which have been utilized to generate virtual particles with desired characteristics [21,22]. However, in the FS-based particle model proposed by Lai et al.

✉ Zhengshou Lai
laizhengsh@mail.sysu.edu.cn

[1] School of Intelligent Systems Engineering, Sun Yat-sen University, Shenzhen 518107, China

[2] School of Aeronautics and Astronautics Engineering, Sun Yat-sen University, Shenzhen 518107, China

[3] Department of Civil and Environmental Engineering, The Hong Kong University of Science and Technology, Hong Kong, China

Published online: 16 November 2021

[14], as well as its recent extension to concave particles [15], the conventional geometric characteristics-based algorithms are adopted to detect particle contacts and resolve contact geometric features. Although the FS-based particle model has shown to be efficient comparing with the clump-based particle model, its application is limited as the geometric characteristics-based contact algorithms are still computationally expensive. In addition, it is not straightforward to incorporate the FS-based particle model with other conventional particle models (e.g., the circular, ellipse-based or polybézier-based particle models).

The Gilbert–Johnson–Keerthi (GJK) algorithm, first proposed by Gilbert et al. [23], is an accurate and efficient algorithm for determining whether two convex objects are in contact, and computing the separation distance if they are not. It was first adopted by Wachs et al. [24] to deal with the contact detection and resolution problem in DEM. By using a glued-convex-particles approach, it was also enabled to handle non-convex particles in a recent study [25]. One of the most attractive features of GJK is that it is applicable to any shape that implements a support function. For example, based on the GJK framework, some versatile particle models have been developed with recourse to poly-super-ellipsoid [26] or polybézier curves [16]. In view of the efficiency and flexibility of GJK, this work is devoted to extending the previous FS-based particle model to the GJK-based contact detection and resolution framework for DEM. A major novelty of this work is that, instead of representing particle surface, the FS is proposed to represent the support function of a particle. Particle surface and support points are then derived based on the FS support function. Hence, the new FS-based particle model is palatable to the GJK-based contact detection and resolution framework and compatible with other conventional particle models in a DEM simulation.

In the following, the methodology, including the FS-based support mapping and convexity constraint, of the new FS-based particle model is first presented in Sect. 2. Then, the performance of the FS-based particle model for describing irregular-shaped particles and for DEM simulations is investigated in Sect. 3. Lastly, concluding remarks are summarized in Sect. 4. The discussion of this work will be limited to two dimensions. The extension of FS to the three dimensions is spherical harmonics [27], where a major challenge for its integration with GJK is the convexity issue. While there exists a closed-form criterion [28] for the spherical harmonics coefficients to achieve a convex particle shape, adjusting the spherical harmonics coefficients to satisfy this criterion is difficult and is one of the major problems to be working on.

2 Methodology

2.1 Review of the original FS-based particle model

In the original FS-based particle model [14], the FS is employed to describe the surface of a particle, as shown in Fig. 1a. With particle surfaces described by FS, the contact detection and resolution are then converted into constrained optimization problems. As depicted in Fig. 1b, point A_p is a surface point of Particle p. The line passing the centroid C_q of Particle q and point A_p would intersect with the surface of Particle q at point A_q. Hence, the contact detection becomes equivalent to determining whether line segment C_qA_p is shorter than line segment C_qA_q, i.e., to finding the minimal of the signed length of A_pA_q. Once a contact is identified, the contact resolution procedure is invoked to evaluate the contact geometric features, such as contact normal, contact overlap and contact point, which are required by a contact model to calculate contact forces. Fig. 1c illustrates the definition of contact geometric features in the original FS-based particle model, where a critical step is to find the intersections (i.e., points I_1 and I_2) of the two particle surfaces.

The original FS-based particle model assumes particle are convex so that the optimization problems of contact detection and resolution can be solved in a global sense using the Newton's method. If concave particles are involved, the contact detection and resolution problem needs to be solved locally for each convex segments of the particles. A recent progress along this line is the work of Su and Wang [15], where the node-to-curve algorithm is employed to detect contacts. As shown in Fig. 1e, particles are first discretized into a set of nodes and the contact detection problem becomes equivalent to determining if there exists a node in particle p that intrudes into particle q. The contact resolution problem is then solved by calculating the overlapping area of the two particle surfaces. In both the original FS-based particle model [14] and the concave extension [15], the contact detection and resolution algorithms are developed based on the geometric characteristics of two particles and the Newton's method. Although the original FS-based particle model is shown to be efficient comparing with the clump-based particle, its application is limited as the geometric characteristics-based contact algorithms are still relatively computationally expensive. In addition, it is not straightforward to incorporate the original FS-based particle model with other particle models in a DEM simulation.

2.2 The new FS-based particle model

In the new FS-based particle model, the FS is employed to describe the support function, which represents the functional relationship between support points and support directions. As shown in Fig. 2a, given a direction $\mathbf{v}$, the corresponding

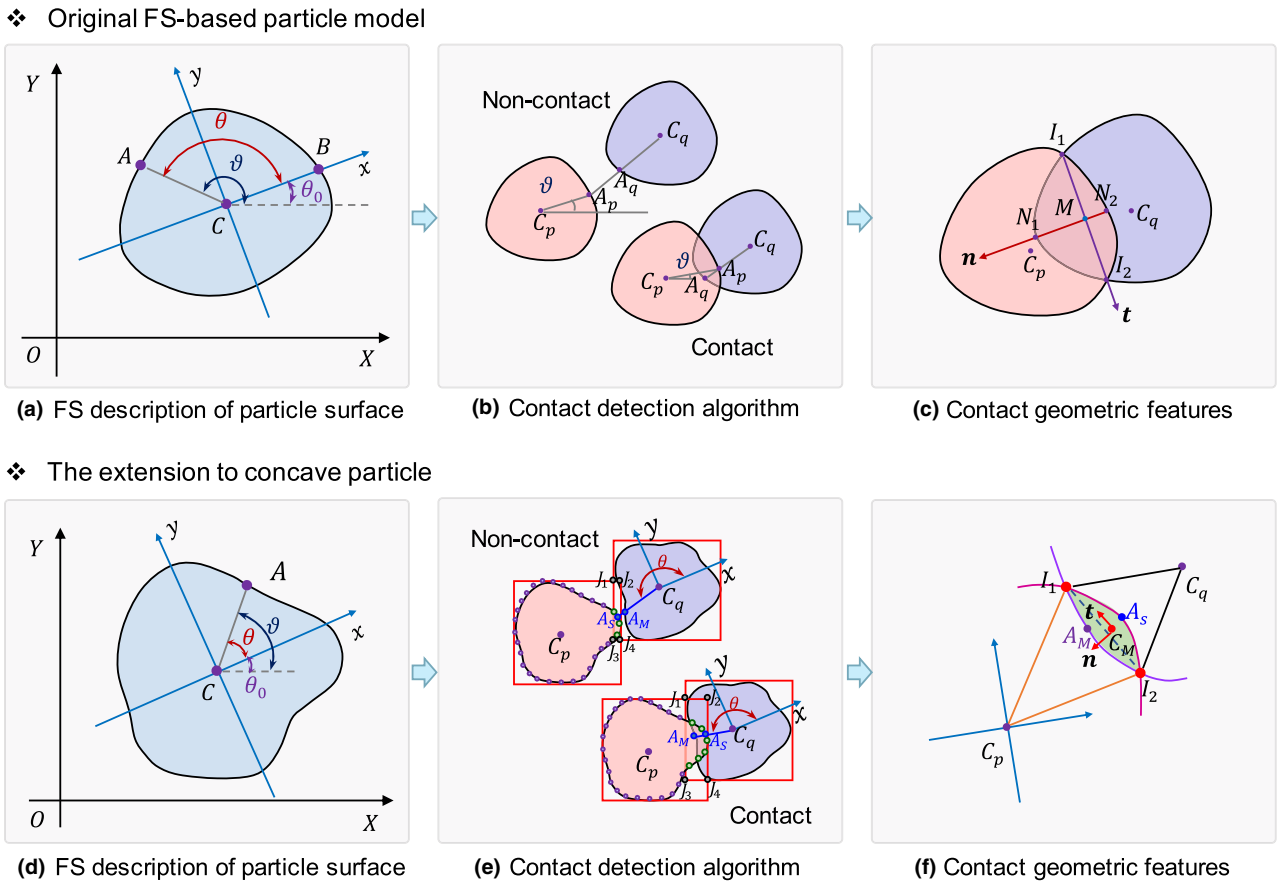

Fig. 1 Illustration of the main methodology of the original FS-based particle models

support point **P** is the surface point that has the maximum dot product with this direction. The support function is then defined as the dot product of the support point and the support direction, such that

$$p(\mathbf{v}) = \max(\mathbf{v} \cdot \mathbf{P}),\ \mathbf{P} \in A \tag{1}$$

In two dimensions, it is convenient to represent the support direction by polar angle θ, that $\mathbf{v} = (\cos\theta, \sin\theta)$. As such, the support function can be expressed as a function of variable θ and can be written in FS as

$$p(\theta) = \frac{1}{2}a_0 + \sum_{n=1}^{N}[a_n \cos(n\theta) + b_n \sin(n\theta)] \tag{2}$$

where a_0, a_n and b_n are the FS coefficients of the support function and should be distinguished from the FS coefficients of radial distance function in the original FS-based particle model [14]; N indicates the FS order and n is the order index. The FS coefficients of radial distance function and support function are implicitly associated with each other for a given shape, while an explicit relationship or correlation between them does not exist. Fig. 2b illustrates the profile of a support function. For a continuous surface, the support direction is perpendicular to the tangent line passing the support point, as shown in Fig. 2c. This feature provides a convenient way to calculate the support point based on the support function, such that [28]

$$x(\theta) = p(\theta)\cos\theta - p'(\theta)\sin\theta \tag{3}$$

$$y(\theta) = p(\theta)\sin\theta + p'(\theta)\cos\theta \tag{4}$$

where $x(\theta)$ and $y(\theta)$ are the coordinates of the support points; $p'(\theta)$ is the derivative of $p(\theta)$ with respect to θ.

With the formulation of support points, the new FS-based particle model is hence palatable to the GJK-based contact detection and resolution framework for DEM simulation. The GJK-based algorithms for contact detection and resolution are well-developed and will not be exhaustively presented in this work. Interested readers are referred to Lai and Huang [24],Wachs et al. [26], Zhao and Zhao [29],Seelen et al. [16] for more details. In this work, the classical GJK and expanding polytope algorithm (EPA) are adopted for the example DEM simulation. There are also improved GJK-

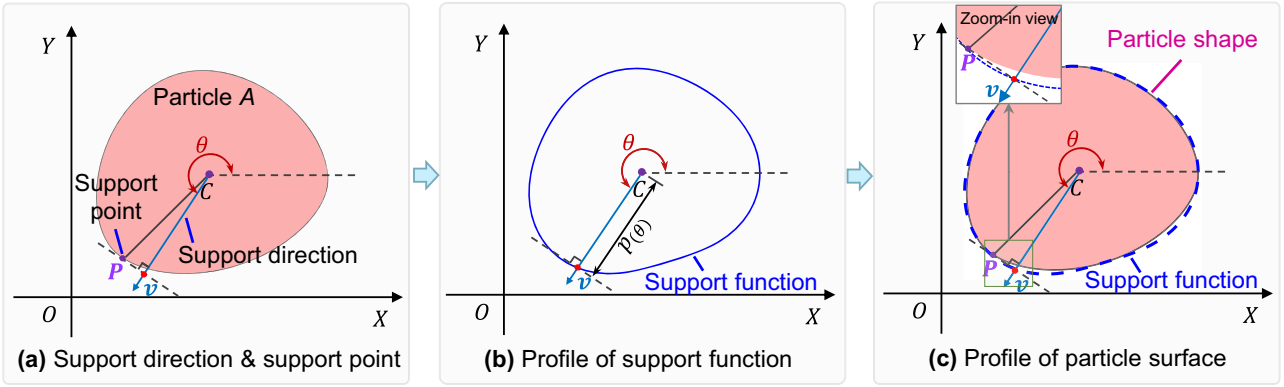

Fig. 2 Illustration of the new FS-based particle model with the definition of support direction, support point and support function

based contact algorithms (e.g., hybrid Levenberg–Marquardt and GJK-erosion approach [26]) with higher performance than the adopted GJK and EPA algorithms. The classical GJK and EPA algorithms are adopted for simplicity, and it is noted that the proposed new FS-based particle model is applicable to those improved algorithms.

2.3 Particle generation and convexity

The procedure for generating particles using the new FS-based particle model is illustrated in Fig. 3. Give a reference shape (which could be obtained from imaging techniques), the boundary points of the shape are first extracted using image processing techniques. The boundary points form a close surface and are made convex by extracting the convex hull. Then, one can sample a uniform set of support directions and calculate the corresponding support function values based on the definition given in Eq. (1). Specifically, for a given support direction, the dot products of all boundary points of the particle with the support direction are calculated, and the boundary point that gives the maximum dot product is the support point corresponding to the given support direction. Finally, the support directions and support function values are cast into Eq. (2) to form an equation array, based on which the FS coefficients can be solved. Once the FS coefficients are solved, they can be cast into Eqs. (3) and (4) to calculate support points, which can be used for particle shape visualization and GJK-based contact detection and resolution.

It is worth mentioning that particle shape can also be represented by using directly the convex polygon (i.e., convex hull) formed by the set of points discretizing the particle surface. Comparing with polygon, the FS-based particle shape description has two advantages. First, the computation of support point for FS is $O(1)$ time complexity (by the virtue of explicit expression of support point), while it is at least $O(\sqrt{n})$ for polygon, where n is the number of polygon vertices. Although the computation of dot product is efficient, the time cost for computing $\sqrt{n}$ times of dot products could be significant for polygons with a large number of vertices, i.e., a smooth shape. Second, the FS coefficients of a particle are closely correlated with the morphological characteristics (e.g., aspect ratio, roundness and roughness) of the particle, which can be utilized to perform shape analysis and to create virtual particles [30].

The precondition of the GJK-based framework for contact detection and resolution is that all particles must be convex. Although the reference shape is made convex when used to generate a FS-based particle, the convexity might not be preserved after the surface sampling and fitting process. An advantage of the new FS-based particle model is that there exists an explicit closed-form expression of convexity condition, given as [28,31]

$$p''(\theta) + p(\theta) \geq 0 \tag{5}$$

where $p''(\theta)$ is the second derivative of $p(\theta)$ with respect to θ. By substituting with the FS support function given in Eq. (2), the convexity constraint for the FS-based particle model can be expressed as

$$\begin{aligned} & p''(\theta) + p(\theta) \\ &= \frac{1}{2}a_0 - \sum_{n=1}^{N}(n^2-1)[a_n \cos(n\theta) + b_n \sin(n\theta)] \\ &= \frac{1}{2}a_0 - \sum_{n=1}^{N}(n^2-1)\sqrt{a_n^2+b_n^2}\sin(n\theta+\beta_n) \geq 0 \end{aligned} \tag{6}$$

where $\beta_n = \text{atan2}(b_n, a_n)$ are the phase variables. With recourse to the characteristic that the absolute value of sine functions is less than one, a sufficient condition of convexity can be derived from Eq. (6), that

$$\frac{1}{2}a_0 - \sum_{n=1}^{N}(n^2-1)\sqrt{a_n^2+b_n^2} \geq 0 \tag{7}$$

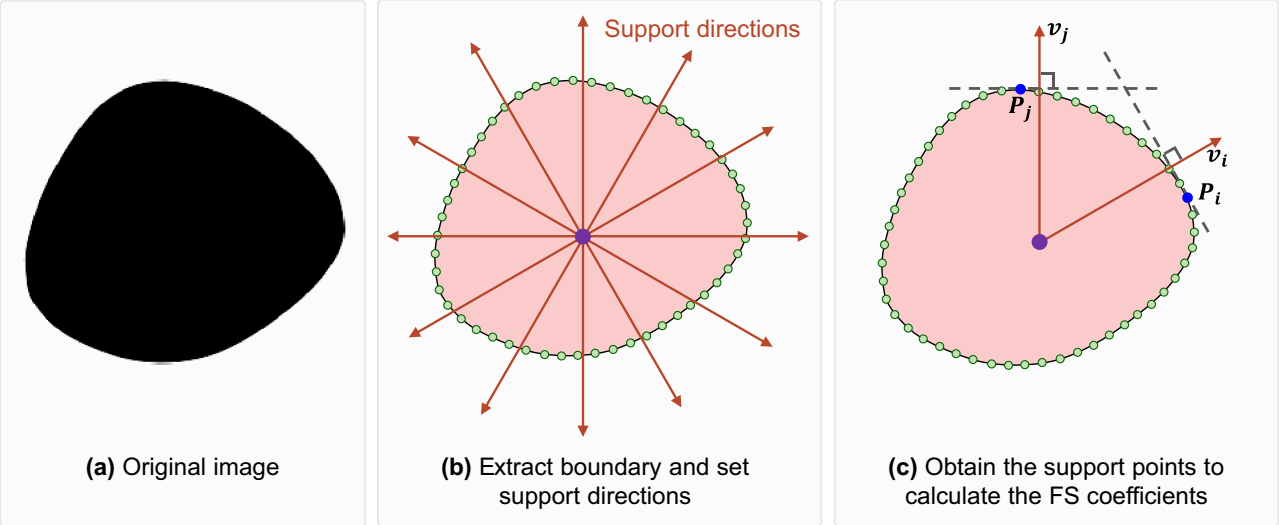

Fig. 3 Illustration of the procedure for generating particle templates using the new FS-based particle model

It can be observed from Eq. (7) that the higher-order FS coefficients, after multiplied by the square term n^2-1, would significantly degrade the convexity condition. In practice, it is proposed to gradually reduce the value of the higher-order FS coefficients, until the convexity condition is satisfied. The coefficients reduction procedure consists of two main steps: (1) select the last two coefficients (i.e., a_n and b_n) that are not negligibly small (i.e., $\sqrt{a_n^2+b_n^2} > \varepsilon$, where ε is the tolerance and is set to 10^{-6} in this work); (2) reduce the selected two coefficients by iteratively multiplying a factor β (i.e., $a_n = \beta a_n$ and $b_n = \beta b_n$). Steps (1) and (2) are repeated until the convexity criterion is satisfied. This approach could be justifiable in that the higher-order FS coefficients are primarily correlated with the surface roughness details of a particle [32]. The surface roughness details are often neglected in a DEM simulation for simplicity and efficiency. As a compensation of the surface roughness effects, a enlarged contact friction is often adopted after calibration. It is worth noting that the shape geometric fitting problem can also be formulated as a constrained minimization problem by taking the shape representation accuracy as objective function and the convexity criterion as constraint. The constrained minimization approach may provide higher shape representation accuracy, comparing with the approach in the present work and will be explored in future for the 3D spherical harmonics case.

3 Numerical examples

This section presents the results of two numerical tests on the new FS-based particle model. The first test involves to apply the new FS-based particle model to describe a set of irregular shapes, where the shape representation accuracy is evaluated and compared with the original FS-based particle model. The second is a random packing and biaxial compression test on particles of various sizes and shapes to demonstrate the performance of the new model in DEM simulation.

3.1 Accuracy in shape representation

To evaluate shape representation accuracy, the new FS-based particle model is applied to 12 shape templates that are previously used in the work of the original FS-based particle model [14]. Similar to the previous work, the percent coverage is used to quantify the shape representation accuracy. The percent coverage is defined as one minus the percent difference between the area covered by the reconstructed FS-based particle and the area covered by the reference shape. There are also researches [33–35] that employ shape characterization descriptors, such as elongation index, flatness index, roundness, roughness, to evaluate the shape representation accuracy. Nonetheless, as these shape characterization descriptors are derived from particle shape profiles, the percent coverage, which directly compares the particle shape profiles of the original shape and the reconstructed shape, is the most basic descriptor for evaluating shape representation accuracy. Figure 4 shows several examples of the FS-based particle shapes with different FS orders. Generally, the new FS-based particle model exhibits a trend of shape evolution similar to the original FS-based particle model with increasing FS order. The shape representation accuracy increases with increasing FS order. Lower-order FS coefficients (e.g., 1 and 2) capture the overall aspect ratios of the particle, whereas higher-order FS coefficients (e.g., 4∼8) affect the roundness of the particle. For non-convex shapes (e.g., template A in

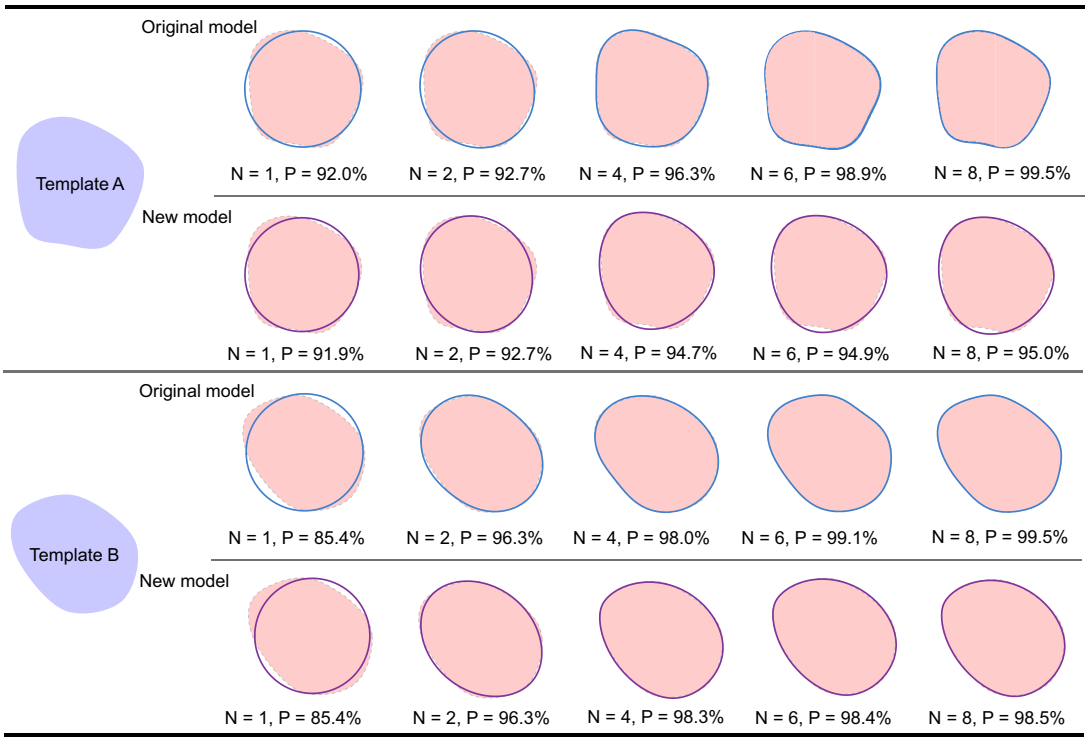

Fig. 4 Examples of FS-based particle shapes with different FS orders

Fig. 4), due to the imposition of convexity during geometric fitting, the new FS method would generally exhibit a shape representation accuracy that is slightly smaller than the original FS method. Whereas for convex shapes (e.g., template B in Fig. 4), the new FS method performs similarly to the original FS method. The slight difference between the two methods (for template B in Fig. 4) is resulted from geometric fitting and numerical errors, and the fact that the FS is employed to represent support points in the new FS method whereas to represent surface points in the original FS method.

As a more quantitative investigation, Fig. 5 plots the evolution of percent coverage with increasing FS order for all the 12 shape templates. The results of the original FS-based particle model are also presented for the purpose of comparison. For the new FS-based particle model, the shape representation accuracy increases with FS order, whereas it maintains at a constant value when the FS order reaches a certain value. As discussed in the previous section, in order to preserve the particle convexity during the geometric fitting process, the value of higher-order FS coefficients is gradually reduced. For some shape templates, the FS coefficients of order 8 or higher are eventually reduced to zeros, and thus the FS-based particle model of order 8 or higher degenerates to a model of order 8. And, for certain shapes, the FS coefficients of order 8 or lower may have to be further reduced to satisfy the convexity constraint, and as a result the FS may even degenerate to an order less than 8. Overall, the shape representation accuracy of the new FS-based particle model is slightly lower (e.g., 95.8% vs. 99.2% for an order of 8) than the original model. Nonetheless, the new model achieves an average percent coverage of more than 95% with an order of 8, which is able to reproduce the overall aspect ratio and roundness of the particles.

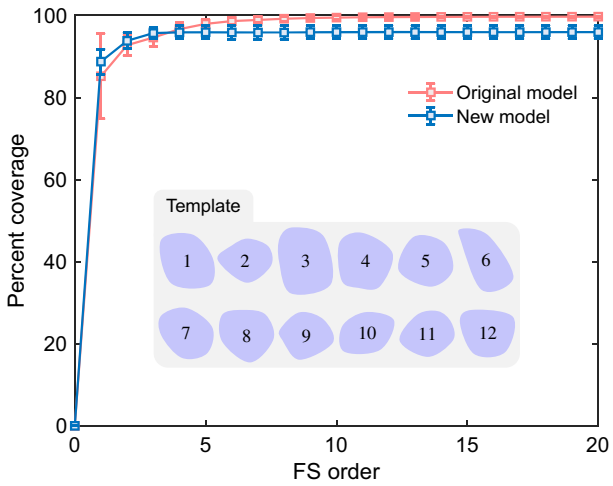

Fig. 5 The evolution of percent coverage with increasing FS order for the original and new FS-based particle model

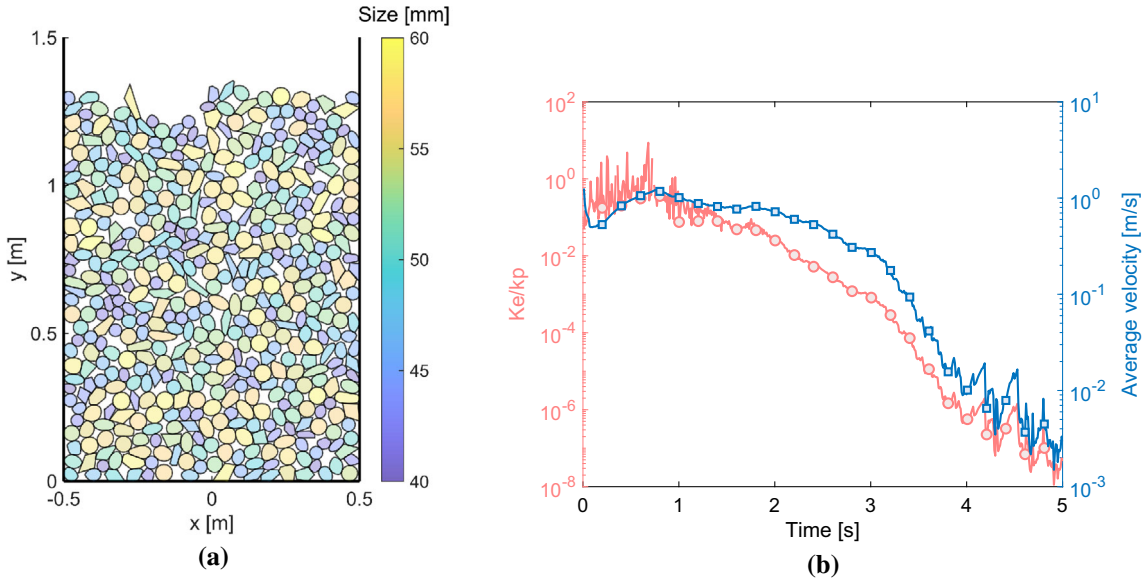

Fig. 6 Results of random packing: **a** snapshot of the particle assembly at the end of random packing, **b** evolution of particle velocity and relative kinetic energy during the packing process

3.2 Random packing and biaxial compression

The random packing and biaxial compression test involves 500 particles that are represented by different particle models, including the circle-, ellipse-, polygon-, polybézier-, and new FS-based particle models. As shown in Fig. 6a, the particle model is randomly selected from the considered models for the generation of each particle. The particles have an equivalent size (i.e., the size of circle with the same area) ranging from 0.04 m to 0.06 m. To begin with, the 500 particles are randomly placed in a rectangle box of 1.0 m in width and 3.0 m in height. These particles are then allowed to settle down at gravity. After reaching quasi-equilibrium, the biaxial compression is performed with two stages, namely the consolidation stage and the compression stage, and with a confining pressure of 100 KPa. The loading rate during the compression stage is 0.1 m/s, which lasts for 2.0 s to account for a final axial strain of about 16%. For simplicity, the linear-spring contact model is used and is given as follows:

$$F_n = k_n \delta_n \tag{8}$$

$$F_t = \min\left(F_t^0 + k_t \Delta\delta_t, \mu_c F_n\right) \tag{9}$$

$$M_c = 0 \tag{10}$$

where F_n and F_t are the contact normal and tangential forces, respectively; k_n and k_t are the contact normal and tangential stiffness, respectively; μ_c is the contact friction coefficient; F_t^0 is the tangential force at the beginning of the current DEM cycle; and M_c is the contact moment. In particular, the contact parameters are listed as follows: normal and tangential stiffness 1×10^7 N/m, contact friction 0.2. The velocity-based damping force and moment [4] are considered with the damping coefficient being 0.7. The timestep is fixed at 1×10^{-4} s. The particle density is 2700 kg/m^3, and the gravity coefficient is 9.8 m/s^2.

A snapshot of the particle assembly at the end of random packing is shown in Fig. 6a. It is observed that the particles are standing by each other, and no particle is unexpectedly overlapping or penetrating into another one. The contacts between the different types of particles are accurately identified. Fig. 6b shows the evolution of the particle average velocity and the relative kinetic energy (the ratio of the kinetic energy to the contact potential energy) during the packing process. Both the average velocity and the relative kinetic energy diminish to a fairly small value at the end of packing process. Fig. 7a plots the evolution of the axial and lateral stresses (compression as positive) of the packing during the biaxial compression process. The lateral stress is successfully maintained at the specified 100 KPa during the whole compression process, whereas the axial stress maintains at 100 KPa during the first second and then gradually increases during the next two seconds. Fig. 7b plots the evaluation of the deviatoric stress ratio and volumetric strain with increasing axial strain (compression as positive). The deviatoric stress ratio increases until the axis strain reaches approximately 6% and then almost plateaus. The volumetric strain increases gradually during whole compression process. Overall, the results of energy evolution, stress evolution and stress-strain behavior indicate the good numerical stability of the new FS-based particle model and DEM simulation.

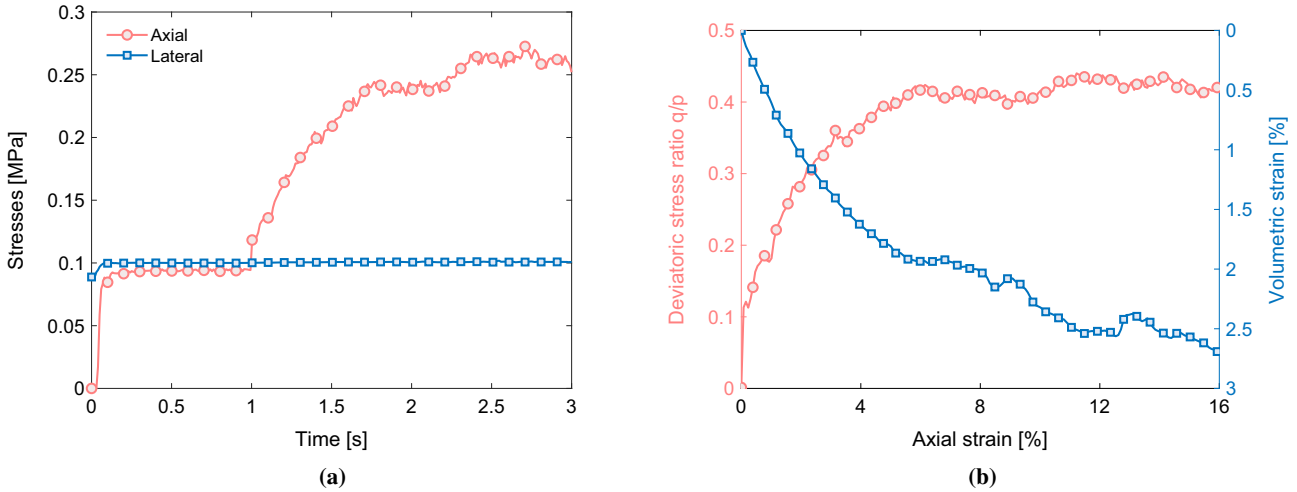

Fig. 7 Evolution of the **a** axial and lateral stresses, and **b** deviatoric stress ratio and volumetric strain during the biaxial compression process

To gain an insight into the computational performance of the new FS-based particle model, the convergence profiles of the GJK and EPA algorithms are plotted in Fig. 8. It can be observed that the pairs of particles that are in contact overall require a larger number of calls for support function than the pairs of particles that are not in contact. For FS-FS particle pairs, the average number of support function calls is 6.4 for contact cases and is 1.0 for non-contact cases. The EPA exhibits a linear convergence rate, which is consistent with observation of the polybézier-based particle model [16]. More specifically, the residual approximately decreases by an order of 10^6 with 10 iterations. Herein, the residual is calculated as the difference between the Euclidean length of the newly added support point and the smallest distance from the origin to the edges of the polytope. As a comparison of the GJK performance for different particle models, the average number of support function calls for different types of particle pair is summarized in Table 1. Overall, the number of support function calls of the new FS-based particle is close to that of the polybézier-based particle models, which have smooth and continuous geometries. The polygon-based particle model requires the least number of support function calls. This finding is consistent with the observation in three-dimensional DEM simulations that the GJK algorithm works better for polyhedra, which have a limited number of vertices and flat faces, than shapes with curved and smooth surfaces [36]. Nonetheless, the FS-based particle model has the advantage of reproducing general-shaped particles with smooth and continuous surfaces.

Lastly, it is worthwhile mentioning about the computational costs of the original and new FS-based particle model. For the new FS-based particle model, which is incorporated with the GJK-based contact detection and resolution framework, the total time cost is about 15 hours for the whole random packing and biaxial compression process (i.e., 80,000 DEM cycles with one Intel i7-7700 core), whereas it takes more than 29.5 hours for the original FS-based particle model. Overall, the results of random packing and biaxial compression tests demonstrate that the new FS-based can be well integrated into the classical GJK-based contact detection and resolution framework, which could significantly improve the computational efficiency of the FS-based particle model for DEM simulation. In addition, the new FS-based particle can be well incorporated with other convex particle models, which improves the flexibility of a DEM simulation to accommodate the various modeling demands in practice.

4 Summary

This work developed a new FS-based particle model that is applicable to the GJK-based contact detection and resolution framework for DEM simulation. In the new FS-based particle model, the FS is employed to describe the support function of a particle. Particle surface and support point of the particle are then formulated based on the FS-based support function. Moreover, the convexity constraint and the procedure for generating convexity preserving FS-based particles were also developed. With the formulation of support points and preservation of convexity, the new FS-based particle model can be readily integrated into the GJK-based contact detection and resolution framework for DEM simulation. It can also be incorporated with other conventional particle models with convex geometries (e.g., circle, ellipse and polybézier). The accuracy of the new FS-based particle model in describing irregular-shaped particles was analyzed using a set of irregular shape templates. Results indicate that with sufficient FS order, the new FS-based particle model is able to reproduce the overall aspect ratio and roundness of a particle. It achieves a percent coverage of more than 95% with

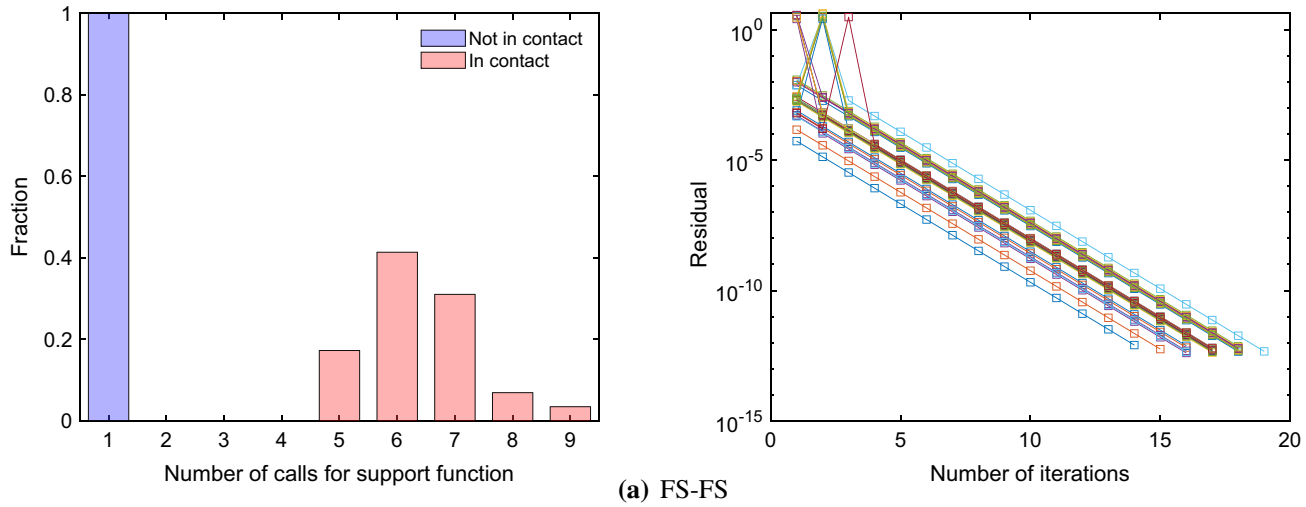

(a) FS-FS

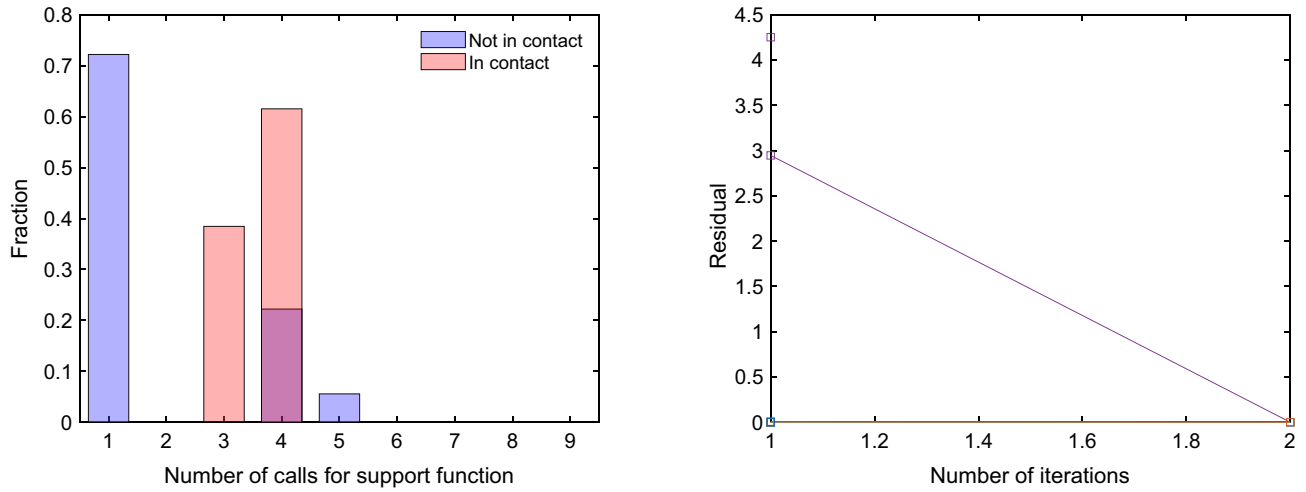

(b) Polygon-Polygon

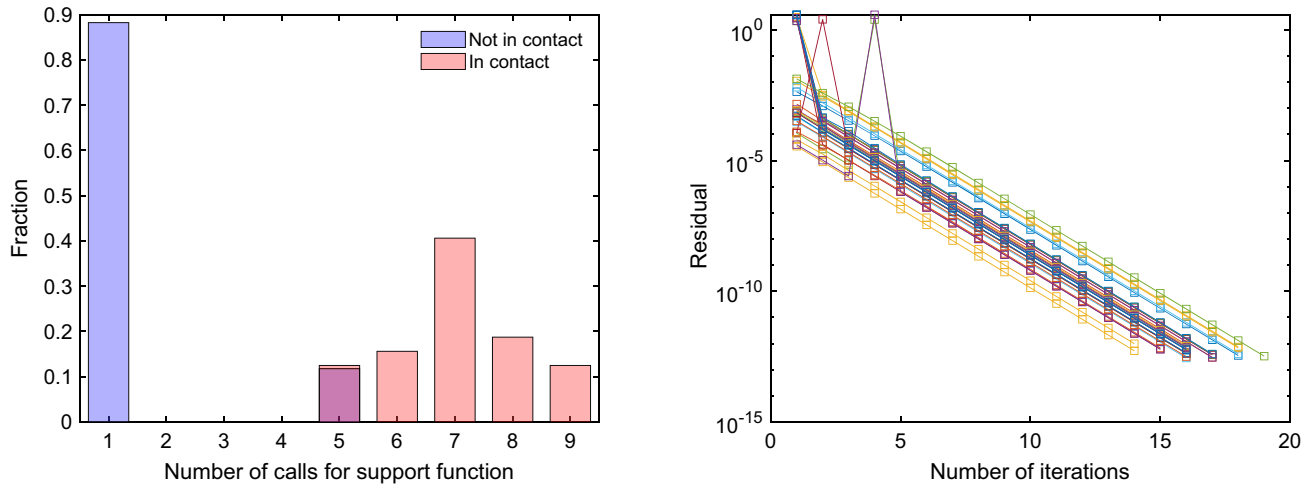

(c) Polybézier-polybézier

Fig. 8 Results of GJK and EPA performance in one DEM computational cycle: **a** FS-FS case, **b** polygon-polygon case, and **c** polybézier-polybézier case. The left column represents the number of support function calls in GJK, and the right column represents the convergence profile of EPA

Table 1 Average number of support function calls in the GJK algorithm for different types of particle pair. The bottom left corner of the table is left out due to symmetry

Particle model	New FS	Circle	Ellipse	Polygon	Polybézier
New FS	4.63	5.51	5.51	4.34	5.46
Circle	–	3.00	6.04	4.52	5.52
Ellipse	–	–	5.20	4.35	5.45
Polygon	–	–	–	2.91	3.92
Polybézier	–	–	–	–	5.10

a FS order of 8. The results of random packing and biaxial compression has demonstrated the good computational efficiency and numerical stability of the new FS-based particle model in DEM simulation. In GJK, the number of support function calls required by the new FS-based particle model is close to that of the other particle models with a smooth and continuous geometry (e.g., polybézier). The EPA for the new FS-based particle model exhibits a linear convergence profile, which is also similar to that of the conventional particle models. Lastly, it is noted that the new FS-based particle model is shown to be two times faster than the original FS-based particle model. The extension of the FS-based particle model to the three dimensions is the spherical harmonics-based particle model, of which the preservation of convexity for GJK is more difficult and will be explored in future.

Acknowledgements This work was financially supported by the National Natural Science Foundation of China (51909289, 51978677, 5201101539), the Shenzhen Natural Science Foundation (JCYJ20190807162401662), and the Shenzhen Science and Technology Project for Sustainable Development (KCXFZ202002011008532).

Declarations

Conflict of interest The authors declare that they have no conflicts of interest.

References

1. Cundall PA, Strack ODL (1979) A discrete numerical model for granular assemblies. Géotechnique 29(1):47–65
2. Ning G, Zhao J (2013) The signature of shear-induced anisotropy in granular media. Comput Geotech 47:1–15
3. Jian G, Nie Z, Zhu Y, Liang Z, Xiang W (2018) Exploring the effects of particle shape and content of fines on the shear behavior of sand-fines mixtures via the DEM. Comput Geotech 106:161–176
4. Andrade JE, Lim KW, Avila CF, Vlahinić I (2012) Granular element method for computational particle mechanics. Comput Methods Appl Mech Eng 241:262–274
5. Hashemi SS, Momeni AA, Melkoumian N (2014) Investigation of borehole stability in poorly cemented granular formations by discrete element method. J Petrol Sci Eng 113:23–35
6. Wachs A (2019) Particle-scale computational approaches to model dry and saturated granular flows of non-Brownian, non-cohesive, and non-spherical rigid bodies. Acta Mech 230:1919–1980
7. Chen Q, Andrade JE, Samaniego E (2011) AES for multiscale localization modeling in granular media. Comput Methods Appl Mech Eng 200(33–36):2473–2482
8. Wu H, Zhao J, Guo N (2019) Multiscale modeling of compaction bands in saturated high-porosity sandstones. Eng Geol 261:105282
9. Cho G, Dodds J, Santamarina J (2006) Particle shape effects on packing density, stiffness, and strength: natural and crushed sands. J Geotech Geoenviron Eng 132(5):591–602
10. Huang Q, Zhou W, Ma G, Mei J, Xu K (2021). Investigation of the grain breakage behaviour of 2D granular materials with disordered pore distribution. *Comput Particle Mechan*,
11. Ting J, Khwaja M, Meachum L, Rowell J (1993) An ellipse-based discrete element model for granular materials. Int J Numer Anal Meth Geomech 17(9):603–623
12. Nassauer B, Liedke T, Kuna M (2013) Polyhedral particles for the discrete element method. Granular Matter 15(1):85–93
13. Lim KW, Krabbenhoft K, Andrade JE (2014) On the contact treatment of non-convex particles in the granular element method. Comput Particle Mechan 1(3):257–275
14. Lai Z, Chen Q, Huang L (2020) Fourier series-based discrete element method for computational mechanics of irregular-shaped particles. Comput Methods Appl Mech Eng 362(5):112873
15. Su D, Wang S (2021) Fourier series-based discrete element method for two-dimensional concave irregular particles. Comput Geotech 132(1):103991
16. Lai Z, Huang L (2021) A polybézier-based particle model for the DEM modeling of granular media. Comput Geotech 134:104052
17. Lu G, Third JR, Müller CR (2015) Discrete element models for non-spherical particle systems: from theoretical developments to applications. Chem Eng Sci 127:425–465
18. Zhong W, Yu A, Liu X, Tong Z, Zhang H (2016) DEM/CFD-DEM modelling of non-spherical particulate systems: theoretical developments and applications. Powder Technol 302:108–152
19. Erlich R, Weinberg B (1970) An exact method for characterization of grain shape. J Sediment Res 40(1):205–212
20. Su D, Yan WM (2018) Quantification of angularity of general-shape particles by using Fourier series and a gradient-based approach. Constr Build Mater 161:547–554
21. Bowman E, Soga K, Drummond W (2001) Particle shape characterisation using Fourier descriptor analysis. Géotechnique 51(6):545–554
22. Koo B, Kim T (2016) Soil particle shape analysis using Fourier descriptor analysis. J Korean Geo-Environ Soc 17(3):21–26
23. Gilbert EG, Johnson DW, Keerthi SS (1988) A fast procedure for computing the distance between complex objects in three-dimensional space. IEEE J Robot Automat 4(2):193–203
24. Wachs A, Girolami L, Vinay G, Ferrer G (2012) Grains3D, a flexible DEM approach for particles of arbitrary convex shape – Part I: numerical model and validations. Powder Technol 224:374–389
25. Rakotonirina AD, Delenne JY, Radjai F, Wachs A (2019) Grains3D, a flexible DEM approach for particles of arbitrary convex shape, Part III: extension to non-convex particles modelled as glued convex particles. Comput Particle Mechan 6(1):55–84

26. Zhao S, Zhao J (2019) A poly-superellipsoid-based approach on particle morphology for DEM modeling of granular media. Int J Numer Anal Meth Geomech 43(13):2147–2169
27. Sun Q, Zheng J (2021) Realistic soil particle generation based on limited morphological information by probability-based spherical harmonics. Comput Particle Mechan 8(2):215–235
28. Antunes P, Bogosel B (2018). Parametric shape optimization using the support function. arXiv preprint arXiv:1809.00254,
29. Seelen L, Padding JT, Kuipers J (2018) A granular discrete element method for arbitrary convex particle shapes: method and packing generation. Chem Eng Sci 189:84–101
30. Mollon G, Zhao J (2012) Fourier-Voronoi-based generation of realistic samples for discrete modelling of granular materials. Granular Matter 14(5):621–638
31. Bayen T, Henrion D (2012) Semidefinite programming for optimizing convex bodies under width constraints. Opt Methods Softw 27(6):1073–1099
32. Zhou B, Wang J, Zhao B (2015) Micromorphology characterization and reconstruction of sand particles using micro X-ray tomography and spherical harmonics. Eng Geol 184:126-137
33. Zhou B, Wang J, Wang H (2018) Three-dimensional sphericity, roundness and fractal dimension of sand particles. Géotechnique 68(1):18–30
34. Zhao L, Zhang S, Huang D, Wang X, Zhang Y (2020) 3D shape quantification and random packing simulation of rock aggregates using photogrammetry-based reconstruction and discrete element method. Constr Build Mater 262:119986
35. Wang X, Yin Z, Su D, Wu X, Zhao J (2021). A novel approach of random packing generation of complex-shaped 3D particles with controllable sizes and shapes. *Acta Geotechnica*, pages 1–22,
36. Feng YT, Tan Y (2019) On Minkowski difference-based contact detection in discrete/discontinuous modelling of convex polygons/polyhedra. Eng Comput 37(1):54–72